

RESEARCH

Open Access



Suppression of microtubule acetylation mediates the anti-leukemic effect of CDK9 inhibition

Xi Xie^{1†}, Baoyuan Zhang^{1†}, Donghe Li¹, Jiaming Gao¹, Jiaoyang Li¹, Chenxuan Liu¹, Yuqing Dan¹, Pengfei Xu¹, Lei Yan¹, Xu Huang¹, Rui Zhang¹, Yunying Yao¹, Wei Huang¹, Jiawei Nie¹, Xinru Wang¹, Bo Jiao¹, Ruibao Ren^{1,2*} and Ping Liu^{1*}

Abstract

Cyclin-dependent kinase 9 (CDK9) is a crucial component of transcription and potential target for anti-cancer therapies, particularly for hematological malignancies. However, the precise mechanisms underlying the therapeutic effects of CDK9 inhibitors remain not fully understood. Here, we found that inhibiting CDK9 either pharmacologically or through gene downregulation, significantly reduced the levels of α -tubulin protein in a time- and dose-dependent manner. We further discovered that CDK9 inhibition led to increased susceptibility of α -tubulin to proteasomal degradation due to reduced acetylation at lysine 40 (K40), an important modification for microtubule stability. An acetylation-mimicking mutant of α -tubulin mitigated the anti-tumor effects of CDK9 inhibition. Mechanically, we identified that CDK9 inhibition downregulated the expression of ATAT1, the acetyltransferase responsible for α -tubulin acetylation, further compromising microtubule stability. We also conducted in vivo studies in a leukemic xenograft model, where AZD4573 treatment led to significant tumor regression, decreased ATAT1 expression, and α -tubulin degradation. Our study unravels a novel molecular mechanism by which CDK9 inhibition disrupts α -tubulin stability and provides valuable insights for exploring effective treatment regimens involving CDK9 inhibitors.

Keywords CDK9, Microtubule acetylation, ATAT1

Introduction

The cyclin-dependent protein kinase 9 (CDK9) is one of the most important transcription regulatory members of the CDK family. In combination with its cyclin partner cyclin T1, CDK9 forms the positive transcription elongation factor b (P-TEFb) complex, which controls the expression of a wide range of eukaryotic genes involved in essential cellular processes through phosphorylation of serine 2 (pSer2) residues in the C-terminal domain of RNA polymerase II (RNAP II) [1–3].

Dysregulated CDK9 signaling has been implicated in the pathogenesis and progression of various cancers,

[†]Xi Xie and Baoyuan Zhang contributed equally to this work.

*Correspondence:

Ruibao Ren

rbren@sjtu.edu.cn

Ping Liu

liuping@shsmu.edu.cn

¹Shanghai Institute of Hematology, State Key Laboratory for Medical Genomics, National Research Center for Translational Medicine at Shanghai, Collaborative Innovation Center of Hematology, Ruijin Hospital, Shanghai Jiao Tong University School of Medicine, Shanghai, China

²International Center for Aging and Cancer, Hainan Medical College, Haikou, Hainan Province, China



especially hematologic malignancies [4, 5]. This finding, coupled with the higher expression of CDK9 in hematological malignancies compared to solid tumor cells, suggests that a highly selective CDK9 inhibitor holds promise as a potential target in acute leukemia therapy [6, 7].

AZD4573 is a novel, highly selective CDK9 inhibitor that binds quickly to its target. The efficacy and safety were evaluated in patients with relapsed/refractory acute myeloid leukemia (AML) and acute lymphoblastic leukemia (ALL) [8]. We found that AZD4573 effectively reduced α -tubulin levels in AML cells in a time- and dose-dependent manner. This finding highlights a previously unrecognized connection between CDK9 and microtubule regulation, which has not been reported before.

Microtubules are crucial components of the cellular cytoskeleton composed of 13 α - β -tubulin dimers (protofilaments) and play fundamental roles in cell division, intracellular transport, and maintenance of cell shape [9–12]. They are also important targets for anticancer drugs, such as paclitaxel and vinblastine, which disrupt microtubule dynamics and exhibit broad effectiveness against hematological malignancies and solid tumors [7, 13, 14].

For microtubules to perform such diverse functions, the cell uses a variety of posttranslational modifications (PTMs) including acetylation, detyrosylation, polyglycylation, polyglutamylolation, and phosphorylation to fine-tune their function [15, 16]. PTMs influence the lifetimes and dynamics microtubule by altering either their physical properties or their interaction with microtubule binding proteins [17].

Distinct from other known microtubule PTMs, acetylation at Lys-40(K-40) of α -tubulin is the only modification that occurs on the luminal side of microtubules [18, 19]. Acetylated tubulins are abundant in long-lived, stable microtubules, and are involved in cellular trafficking, ciliogenesis, cell motility, and ontogeny. Aberrant tubulin acetylation has been implicated in neurodegenerative disorders, ciliopathies, and cancers [20, 21].

Lys-40(K-40) of α -tubulin was identified as a reversible PTM. The primary enzyme responsible for microtubule acetylation has been identified as α -tubulin acetyltransferase (α TAT1) [22, 23], and the α K40 acetylation is removed by two enzymes: the histone deacetylase 6 (HDAC6) [24] and sirtuin 2 (SIRT2) [25].

In this study, we found that CDK9 inhibition downregulated the expression of the α -tubulin acetyltransferase ATAT1 in AML cells, leading to a decrease in α -tubulin acetylation at the K40, affecting microtubule stability and making α -tubulin more prone to degradation. This work indicates that modulation of α -tubulin acetylation through CDK9 inhibition may constitute a novel and potentially effective therapeutic strategy in combating

tumor progression, highlighting the significance of further exploration into the detailed mechanisms.

Results

CDK9 inhibition leads to a reduction in α -tubulin

CDK9 plays a critical role in the onset and progression of tumors. Several CDK9 inhibitors have entered clinical trial stages, demonstrating potential therapeutic potential. However, the mechanisms by which CDK9 inhibition exerts its effects needs further investigation for enhancing efficacy, reducing toxicity, and decreasing drug resistance in clinical applications.

We treated MOLM-13 and MV4-11 AML cells with AZD4573 and observed a significant decrease in α -tubulin levels in a dose-dependent manner, while the reference protein β -actin did not exhibit distinct changes, ruling out the possibility that the decrease in α -tubulin levels was a consequence of cell death (Fig. 1A-B). Immunofluorescence staining revealed that α -tubulin was primarily situated in the cytoplasm and exhibited a particular polarity or orientation. However, after treatment with AZD4573, a notable decrease was observed in the cytoplasmic fluorescence intensity of α -tubulin (Fig. 1C).

To access the generalizability of our findings, we expanded our experiments to ALL cell lines, SUP-B15 and RS4-11, where observed similar reductions in α -tubulin levels following AZD4573 treatment (Figure S1A-B). Additionally, another highly selective CDK9 inhibitor, JSH-105, also induced a reduction in α -tubulin in AML cells (Figure S2A-B), suggesting that these effects are consistent across different CDK9 inhibitors.

Furthermore, to confirm that suppression of CDK9 gene expression alone could replicate these effects, we established stable CDK9 knockdown cell lines (sh-CDK9-1, sh-CDK9-2) and a control cell line (sh-NC) in MOLM-13, MV4-11 cells. Upon CDK9 knockdown, we detected a significant decrease in α -tubulin levels in all these cells (Fig. 1D-E).

All these results suggest that reduced α -tubulin is indeed a consequence of CDK9 inhibition rather than off-target effects of CDK9 inhibitors.

These observations reveal that CDK9 inhibition impacts α -tubulin stability, suggesting a novel mechanism of CDK9 inhibitors in cancer treatment. Although many biological roles of CDK9 have been studied, there is currently no literature reporting the relationship between CDK9 and microtubules. Further investigation is required to elucidate whether inhibiting CDK9 affects the structure and function of cellular microtubules, and whether this effect contributes to the partial anticancer mechanism of CDK9 inhibitors.

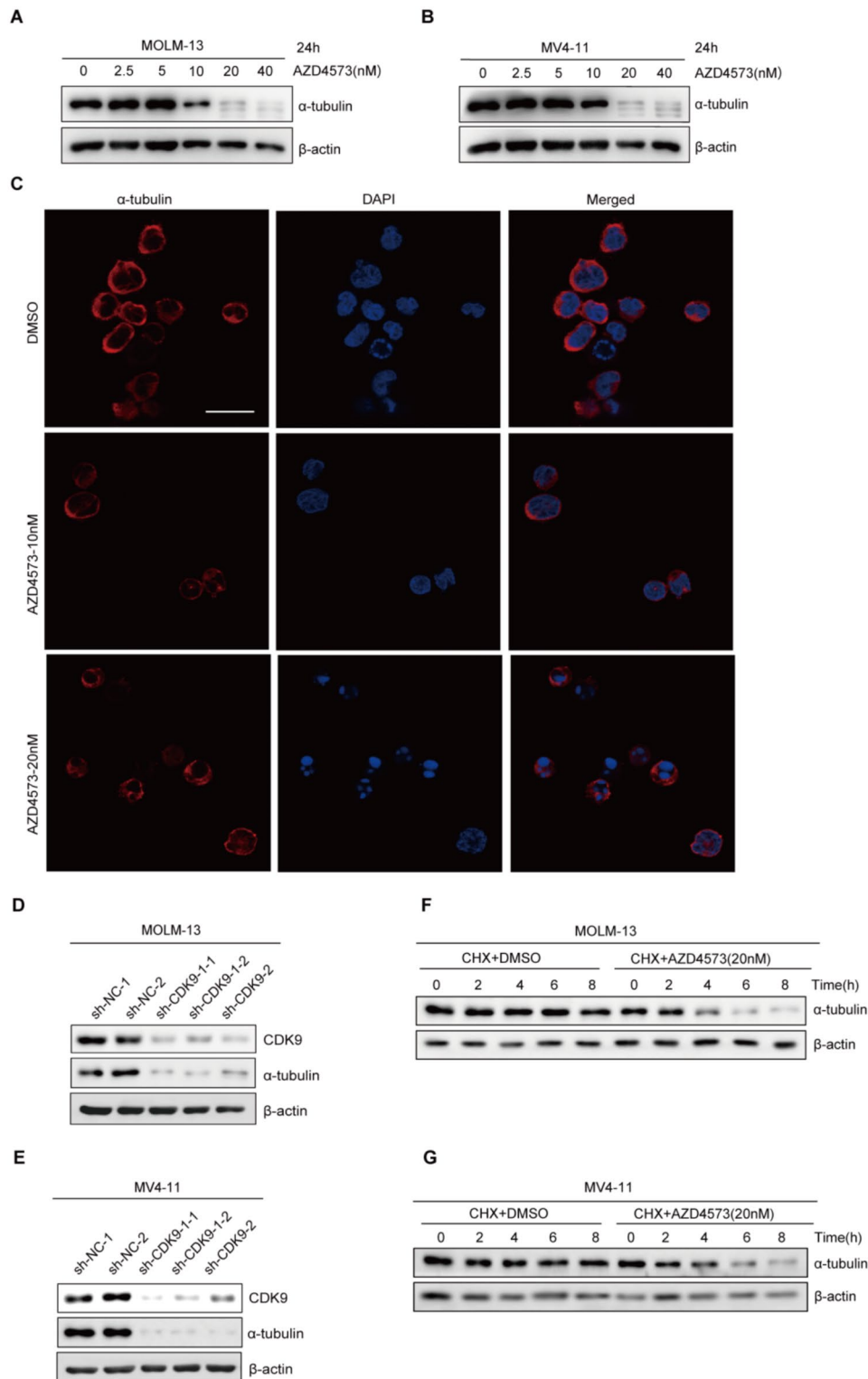


Fig. 1 CDK9 inhibition leads to a reduction in α -tubulin. MOLM-13 cells (**A**) and MV4-11 cells (**B**) were treated with AZD4573 at different concentrations for 24 h, the levels of α -tubulin and other proteins were detected by Western Blot; (**C**) MOLM-13 cells were treated with DMSO or AZD4573 at various concentrations for 24 h and the expression of α -tubulin was detected. Red fluorescence indicates α -tubulin, and blue fluorescence indicates the nucleus. The scale bar is 36.8 μ m; (**D-E**) After MOLM-13 cells (**D**), MV4-11(**E**) stably transfected with sh-NC, sh-CDK9-1, and sh-CDK9-2, the knockdown efficiency of CDK9 was detected by Western Blot, and the level of α -tubulin was detected; MOLM-13 (**F**) and MV4-11 cells (**G**) were treated with CHX (final concentration of 10 μ g/mL) in the presence or absence of AZD4573 at a concentration of 20 nM for different time courses. The levels of α -tubulin were detected by Western Blot

The metabolism of α -tubulin is modulated by CDK9 inhibition

Given that CDK9 might regulate the protein stability of α -tubulin, we first treated MOLM-13 cells with 10 μ g/mL of Cycloheximide (CHX) to inhibit new protein synthesis, following by 20 nM AZD4573. Remarkably, we noticed a substantial reduction in α -tubulin levels in the CHX+AZD4573 treatment group (Fig. 1F), indicating that AZD4573 significantly accelerated the degradation of α -tubulin. We conducted similar experiments on MV4-11, and detected similar effects (Fig. 1G). These results strongly suggested that AZD4573 enhanced the decay of α -tubulin protein in AML cells.

Corroborative evidence from above treatments supported the idea that CDK9 inhibition could influence the metabolic processes of α -tubulin in AML cells.

CDK9 inhibition decreases the α -tubulin acetylation level

Tubulin stability is known to be intrinsically related to various post-translational modifications. Particularly, acetylation of α -tubulin at lysine 40 (K40) is a crucial modification for microtubule stability.

To further dissect the mechanism of CDK9 inhibition leading to α -tubulin degradation, the alterations in acetylated α -tubulin level in MOLM-13 cells after AZD4573 treatment were assessed. We noted that acetylated α -tubulin gradually reduced with increasing concentration of AZD4573 at 6 h, while a distinct α -tubulin decreased later, suggesting the reduction of acetylated α -tubulin precedes α -tubulin degradation (Fig. 2A-C). These findings propose that AZD4573 might initially decrease α -tubulin acetylation, inducing microtubule instability, and ultimately leading to degradation. Similar observations were made in MV4-11 (Fig. 2D-F), SUP-B15 (Figure S1A) and RS4-11 (Figure S1B) cells. Additionally, the selective CDK9 inhibitor JSH-105 also reduced acetylated α -tubulin levels in a dose-dependent manner in MOLM-13 and MV4-11 cells (Figure S2A-B), demonstrating that these effects are consistent across different CDK9 inhibitors.

Furthermore, after treating MOLM-13 cells with AZD4573 (10 nM) for 24 h, an immunofluorescence staining displayed that the chromosomes in the AZD4573-treated cells were significantly condensed, tangled, and disorderly arranged compared to the control. The green fluorescence, indicative of acetylated α -tubulin, was notably weakened, while the red fluorescence representing α -tubulin lost its regular polar distribution and became diffuse (Fig. 2G).

In order to further corroborate whether CDK9 inhibition leads to reduced α -tubulin acetylation, we engineered stable cell lines with CDK9 knockdown in both MOLM13 and MV4-11 cells, namely sh-CDK9-1, sh-CDK9-2, and a control sh-NC. We observed that the

level of acetylated α -tubulin was notably decreased in the CDK9 deficiency cells (Fig. 2H, I).

These observations fortify our conclusion that CDK9 inhibition initiates α -tubulin degradation by reducing the level of α -tubulin acetylation.

CDK9 inhibition exerts its anti-tumor effects by reduction α -tubulin acetylation

While we have discovered that CDK9 inhibition reduced the acetylation level of α -tubulin, leading to tubulin degradation in leukemia cells, it is critical to further verify whether this reduction in α -tubulin acetylation is indeed a key mechanism through which CDK9 inhibition exerts its biological effects.

To further investigate the relationship between the acetylation of α -tubulin and the pharmacological effects of CDK9 inhibitors, we measured cell proliferation activity of MOLM-13, MV4-11, OCI-AML3, and THP-1 treated with AZD4573 and found that all these cells were relatively sensitive to AZD4573, with no inherent resistance to this drug (data not shown). We selected MOLM-13 and MV4-11 to establish AZD4573-resistant strains, each with an IC₅₀ value five times higher than that of the primary parental cells (Fig. 3A and C). We observed that acetylated α -tubulin levels in MOLM-13 and MV4-11 resistant strains significantly increased compared to their parental cells (Fig. 3B and D). After 6 h of AZD4573 treatment, acetylated α -tubulin levels declined in parental cells but increased in the resistant strains (Fig. 3E, F). Therefore, we can further conclude that the increased level of acetylated α -tubulin can mediate the resistance of leukemic cells to CDK9 inhibition.

Meanwhile, we established stable MOLM-13 cell lines overexpressing utilizing a series of plasmids associated with α -tubulin acetylation: α -tubulin-WT (Wild type), α -tubulin-K40Q, and α -tubulin-K40R (Fig. 4B). Molecular models suggest that the K40Q mutation can imitate acetylation by facilitating the formation of salt bridges between microtubule protofilaments, while K40R may represent a state of acetylation deactivation [26]. Following a 48-hour treatment with AZD4573, cell proliferative vitality assay showed that α -tubulin K40Q could substantially decreased the sensitivity of MOLM-13 cells to AZD4573, while α -tubulin K40R had no effect on the drug sensitivity (Fig. 4A). These experiments were replicated in Hela cells and yield consistent results (Fig. 4E, F). Using PARP cleavage to detect apoptosis, we found that α -tubulin-K40Q could mitigate the apoptosis of MOLM-13 cells induced by CDK9 deficiency, while α -tubulin-K40R could not (Fig. 4C). Consistently, α -tubulin-K40Q can reverse the inhibition of MOLM-13 cell proliferation caused by CDK9 knockdown. (Fig. 4D). These findings suggested that inhibiting CDK9 exerted a biological effect through the reduction of α -tubulin acetylation and

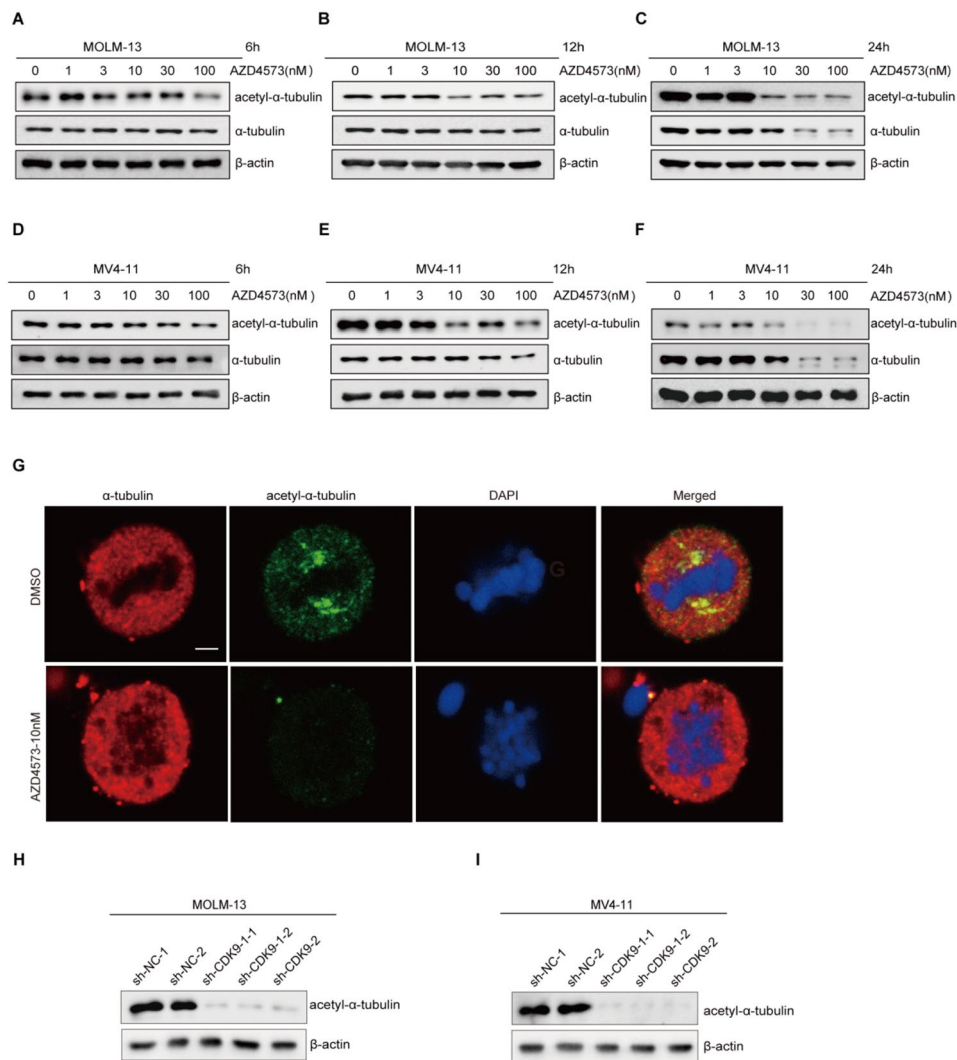


Fig. 2 CDK9 inhibition can degrade α -tubulin by reducing α -tubulin acetylation level. (**A-C**) MOLM-13 cells were treated with AZD4573 at different concentrations (0, 1, 3, 10, 30 and 100 nM) for 6 (**A**), 12 (**B**) and 24 h (**C**), respectively. Western Blot was used to detect the protein levels of acetylated α -tubulin and α -tubulin; (**D-F**) MV4-11 cells were treated with AZD4573 at different concentrations (0, 1, 3, 10, 30 and 100 nM) for 6 (**D**), 12 (**E**) and 24 h (**F**), respectively. Western Blot was used to detect the protein levels of acetylated α -tubulin and α -tubulin; (**G**) MOLM-13 cells were treated with DMSO or AZD4573 10 nM for 24 h and the distribution of α -tubulin, acetylated α -tubulin, and nucleus were observed. Red fluorescence indicates α -tubulin, green fluorescence indicates acetylated α -tubulin, and blue fluorescence indicates the nucleus. The scale bar is 12.3 μ m; (**H-I**) MOLM-13 cells (**H**) and MV4-11 cells (**I**) were stably transfected with sh-NC, sh-CDK9-1, and sh-CDK9-2, the level of acetylated α -tubulin was detected through Western Blot

the cytotoxic effect of CDK9 inhibition can be reversed by restoring the acetylation level.

CDK9 regulates the transcription of α -tubulin acetyltransferase ATAT1

Given that CDK9 inhibition reduces α -tubulin acetylation, we further focused our investigation on the enzymes involved in this process. Specifically, the acetylation of α -tubulin is primarily regulated by the acetyltransferase ATAT1 and deacetylases HDAC6 and SIRT2 [9]. Using qPCR (Table S1), we found that ATAT1 transcription was notably downregulated in MOLM-13, MV4-11, THP-1, and OCI-AML3 cells treated with AZD4573,

while HDAC6 and SIRT2 showed no consistent changes (Fig. 5A-C).

This downregulation was confirmed at the protein level, where ATAT1 levels decreased in a dose-dependent manner (Fig. 5E-F) and also showed a time-dependent reduction (Figure S3A-B). Similar results were observed in ALL cell lines SUP-B15 and RS4-11 (Figure S1C-D) and with the use of another CDK9 inhibitor, JSH-105, in AML cells (Figure S2C-D). Simultaneously, upon stably knocking down CDK9 in MOLM-13 and MV4-11 cells, we observed a significant decrease in ATAT1 (Fig. 5G, H). These results suggest that CDK9 inhibition

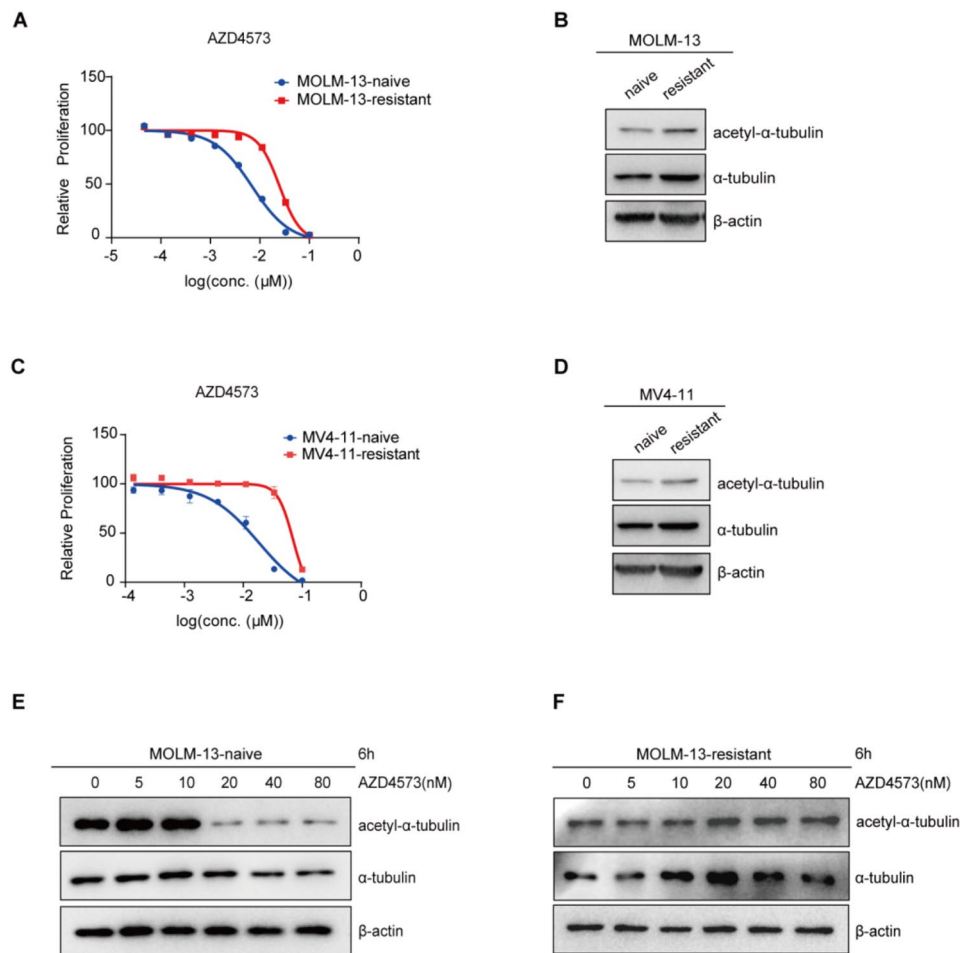


Fig. 3 Acetylated α -tubulin can mediate the resistance of AML cells to CDK9 inhibition. **(A)** MOLM-13 cells were continuously cultured with AZD4573 at increasing concentrations for 6 months. CellTiter-Glo was used to detect the viability of parental cells and resistant cells, and a proliferation curve was drawn; **(B)** Western Blot was used to detect acetylated α -tubulin and α -tubulin in AZD4573 resistant and parental MOLM-13 cell lines; **(C)** MV4-11 cells were continuously cultured with AZD4573 at increasing concentrations for 6 months. CellTiter-Glo was used to detect the viability of parental cells and resistant cells, and a proliferation curve was drawn; **(D)** Western Blot was used to detect acetylated α -tubulin and α -tubulin in AZD4573 resistant and parental MV4-11 cell lines; **(E-F)** MOLM-13 parental cell line **(E)** and resistant cell line **(F)** were treated with various concentrations of AZD4573 for 6 h, and the protein levels of acetylated α -tubulin and α -tubulin were detected through Western Blot

reduces α -tubulin acetylation by downregulating ATAT1 transcription.

To confirm that the effects on α -tubulin were due to ATAT1 downregulation, we conducted a rescue experiment. In MOLM-13 cells stably overexpressing ATAT1 and treated with AZD4573, we observed that acetylated α -tubulin and total α -tubulin levels remained largely unchanged. In contrast, control cells showed significant reductions in both acetylated and total α -tubulin after AZD4573 treatment (Fig. 5I-K). This finding confirms that the effects on α -tubulin are indeed mediated by ATAT1 downregulation.

To further investigate how AZD4573 downregulates ATAT1, we measured the levels of phosphorylated CTD (p-CTD), a key marker of transcriptional activity on RNA polymerase II. CDK9, in complex with Cyclin T1 to form P-TEFb (Positive Transcription Elongation Factor

b), promotes mRNA elongation by phosphorylating the C-terminal domain (CTD) of RNA polymerase II. Inhibiting CDK9 disrupts this process, causing a transient suppression of transcription, particularly affecting short-lived transcripts. Following 6 h of AZD4573 treatment in MOLM-13 cells, we observed a significant decrease in p-CTD levels (Fig. 5D), consistent with this mechanism.

By downregulating ATAT1 in MOLM-13 and MV4-11 cells, we observed a gradually reduction in acetylated α -tubulin levels (Fig. 6A, C). To assess the biological impact of ATAT1 knockdown, we examined proliferation in these cell lines. Our results showed a clear positive correlation between the extent of ATAT1 knockdown and the degree of inhibition of cell proliferation (Fig. 6B, D). This suggested that ATAT1 downregulation plays a crucial role in suppressing leukemic cell growth.

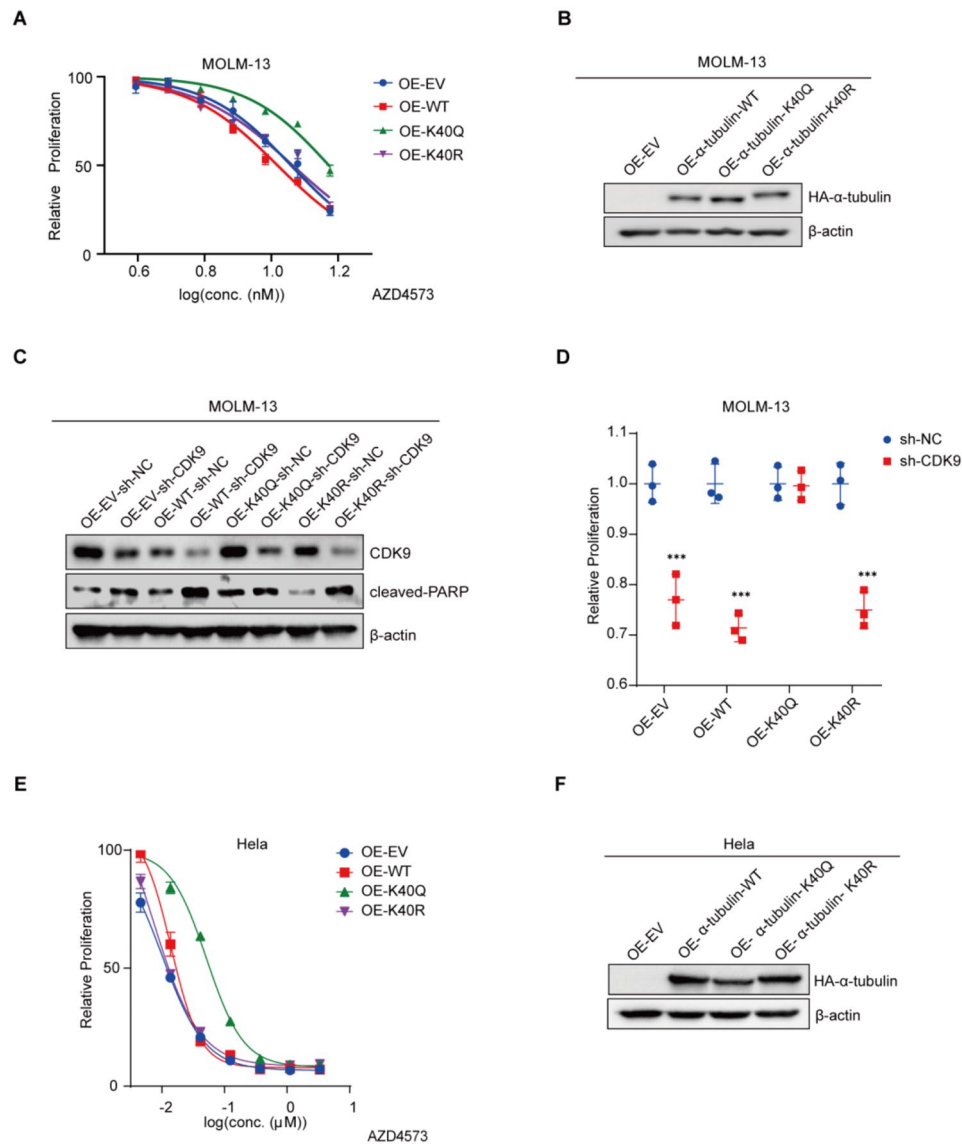


Fig. 4 CDK9 inhibition exerts its anti-tumor effects by reduction α -tubulin acetylation. **(A–B)** MOLM-13 cells stably transfected with EV, α -tubulin-WT, α -tubulin-K40Q (simulated acetylation), and α -tubulin-K40R (simulated acetylation inactivation) plasmids were treated with different concentrations of AZD4573 over 48 h. **(A)** CellTiter-Glo was used to detect the cell viability and draw proliferation curves. **(B)** The efficiency of overexpression was verified by western blot; **(C)** After MOLM-13 cells were stably transfected with an empty vector (EV), α -tubulin-WT, α -tubulin-K40Q, and α -tubulin-K40R plasmids, CDK9 was knocked down, and the CDK9 knockdown efficiency was verified by Western Blot. Additionally, the expression of cleaved-PARP was detected; **(D)** CellTiter-Glo was used to detect the proliferation activity of cells across each group, and a proliferation dot plot was drawn. The P-value was calculated using a t test, $***, P < 0.001$; **(E)** HeLa cells stably transfected with EV, α -tubulin-WT, α -tubulin-K40Q (simulated acetylation), and α -tubulin-K40R (simulated acetylation inactivation) plasmids were treated with different concentrations of AZD4573 over 48 h. CellTiter-Glo was used to detect the cell viability and draw proliferation curves; **(F)** The efficiency of overexpression was verified by western blot

Together, our results indicated that CDK9 inhibition can cause cell death by reducing the level of ATAT1 expression and subsequently leading to α -tubulin degradation.

AZD4573 drives regression of MV4-11 tumor xenografts

AZD4573 has demonstrated reliable safety in vivo and has advanced to clinical trials, showing strong therapeutic potential. To evaluate whether its in vitro activity

translates to in vivo efficacy, we tested AZD4573 in a MV4-11 xenograft model, using an intermittent dosing schedule to achieve the target inhibition identified in vitro. Mice with MV4-11 tumors were treated weekly with 5 mg/kg AZD4573, administered intraperitoneally twice daily for 2 days, followed by 5 days off. This regimen resulted in significant tumor regression without notable weight loss (Fig. 7A–C).

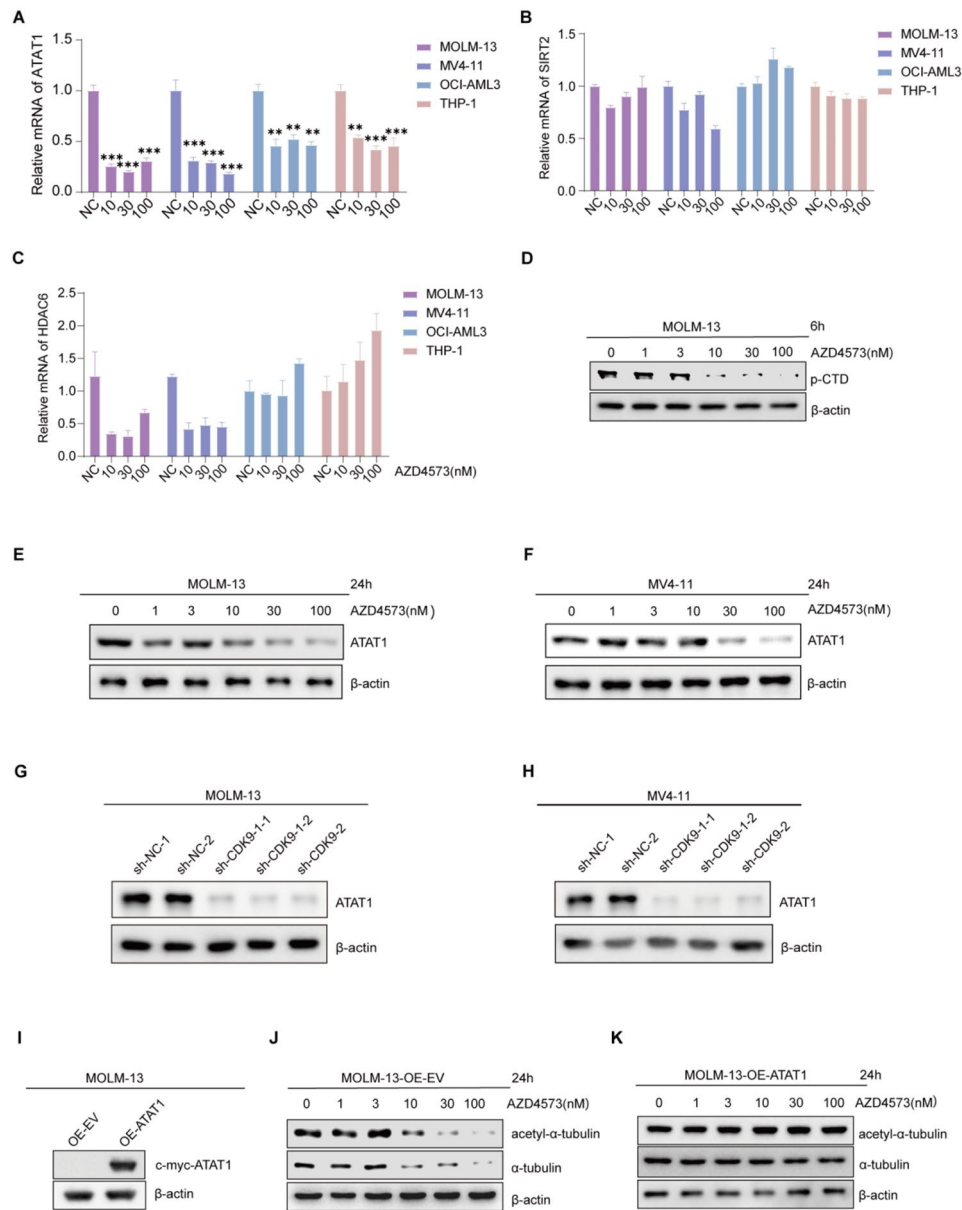


Fig. 5 CDK9 regulates the transcription of α -tubulin acetyltransferase ATAT1. (**A-C**) MOLM-13, MV4-11, OCI-AML3, and THP-1 cell lines were treated with various concentrations of AZD4573 for 4 h. qPCR was used to detect the mRNA changes of α -tubulin acetyltransferase ATAT1 (**A**), SIRT2 (**B**) and HDAC6 (**C**). The P-value was calculated using a t test. **, $P < 0.01$. ***, $P < 0.001$; (**D**) MOLM-13 cells were treated with AZD4573 for 6 h, phosphorylated CTD (p-CTD) level was detected through Western Blot; (**E-F**) MOLM-13 (**E**) and MV4-11 (**F**) cells were treated with various concentrations of AZD4573 for 24 h, the changes of ATAT1 and other proteins were detected through Western Blot; (**G-H**) MOLM-13 cells (**G**) and MV4-11 cells (**H**) were stably transfected with sh-NC, sh-CDK9-1, and sh-CDK9-2, and the protein level of ATAT1 were detected by Western Blot; (**I-K**) MOLM-13 cells stably transfected with EV, ATAT1 overexpressing plasmids were treated with different concentrations of AZD4573 over 24 h. (**I**) The efficiency of overexpression was verified by western blot; (**J-K**) MOLM-13 cells stably transfected with EV (**J**) and MOLM-13 cells stably transfected with ATAT1 overexpressing plasmids (**K**) were treated with various concentrations of AZD4573 for 24 h, the changes of acetylated α -tubulin and α -tubulin were detected through Western Blot

Tumors were harvested on days 2 and 9, 4 h after dosing, to assess the transcription level of ATAT1 and the protein level of α -tubulin. We observed a significant reduction in ATAT1 mRNA levels in the AZD4573-treated group (Fig. 7D), consistent with in vitro findings. Similarly, α -tubulin protein levels in tumor cells were

significantly decreased following AZD4573 treatment (Fig. 7E-F).

In Conclusion, our study reveals a novel mechanism by which CDK9 inhibition leads to a reduction in α -tubulin acetylation and subsequent destabilization of microtubules in leukemic cells. We demonstrated that this process is mediated by the downregulation of

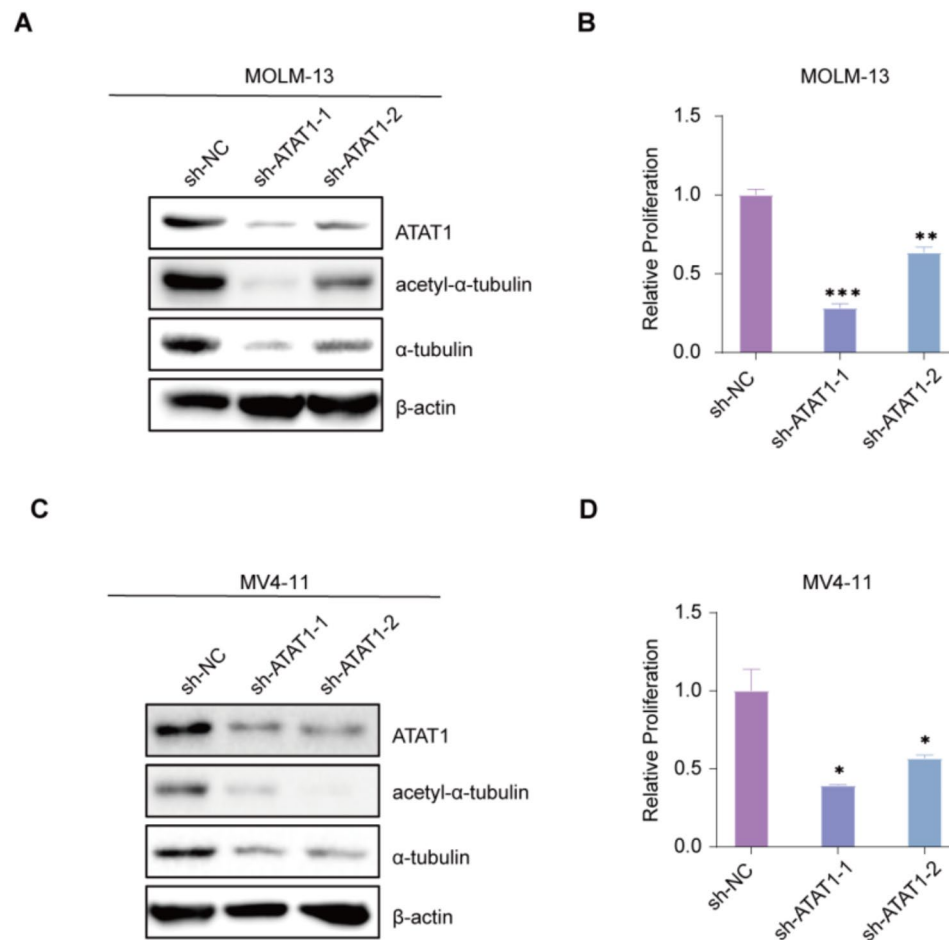


Fig. 6 Downregulation of ATAT1 plays a crucial role in suppressing AML cell growth. **(A)** MOLM-13 cells were stably transfected with sh-NC, sh-ATAT1-1, and sh-ATAT1-2 plasmids, and Western Blot was used to detect the knockdown efficiency of ATAT1 as well as the changes in acetylated α -tubulin and α -tubulin; **(B)** After MOLM-13 cells were stably transformed with plasmids sh-NC, sh-ATAT1-1 and sh-ATAT1-2, CellTiter-Glo was utilized to detect the cell proliferation activity of each cell line and draw bar graphs. The P-value was calculated via a t test, **, $P < 0.01$.***, $P < 0.001$; **(C)** MV4-11 cells were stably transfected with sh-NC, sh-ATAT1-1, and sh-ATAT1-2 plasmids, Western Blot was then used to detect the knockdown efficiency of ATAT1 and the alterations to acetylated α -tubulin and α -tubulin; **(D)** After MV4-11 cells were stably transformed with plasmids sh-NC, sh-ATAT1-1 and sh-ATAT1-2, CellTiter-Glo was used to detect the cell proliferation activity of each cell line and draw a bar graph. The P-value was calculated via a t test, *, $P < 0.05$

the acetyltransferase ATAT1, which directly impacts α -tubulin stability (Fig. 8).

Discussion

CDK9 is a critical kinase regulating gene transcription and is intrinsically associated with the maintenance, growth, metastasis, and drug resistance of tumor cells. Notably, previous research has emphasized its regulation of anti-apoptotic molecules like MCL-1 and MYC, which are critical in the survival and growth of tumor cells [8, 27, 28]. Despite some studies have shown a strong correlation between MCL-1 and the CDK9 inhibitor AZD4573, it was interesting to find tumor cells highly sensitive to the CDK9 inhibitor, yet displaying resistance to MCL-1 inhibition. This indicates that CDK9 may regulate molecules other than MCL-1 [8], hence necessitating further research into other potential targets and

mechanisms of CDK9 both in normal cells and cancerous cells.

In our research, we ventured into exploring this complex mechanism and uncovered a novel interaction between CDK9 and ATAT1, an enzyme integral to tubulin acetylation. Our findings suggested that CDK9 inhibition resulted in downregulation of ATAT1 transcription. This led to a significant reduction in α -tubulin acetylation levels, culminating in microtubule instability and protein degradation. The end effect was inhibition of tumor cell proliferation and induction of apoptosis. The exploration of this novel mechanism provides an exciting potential target for cancer treatment.

ATAT1's function in regulating tubulin acetylation, and subsequently, microtubule stability, has been previously well documented. Nevertheless, our study introduces the concept that CDK9 may modulate this process through

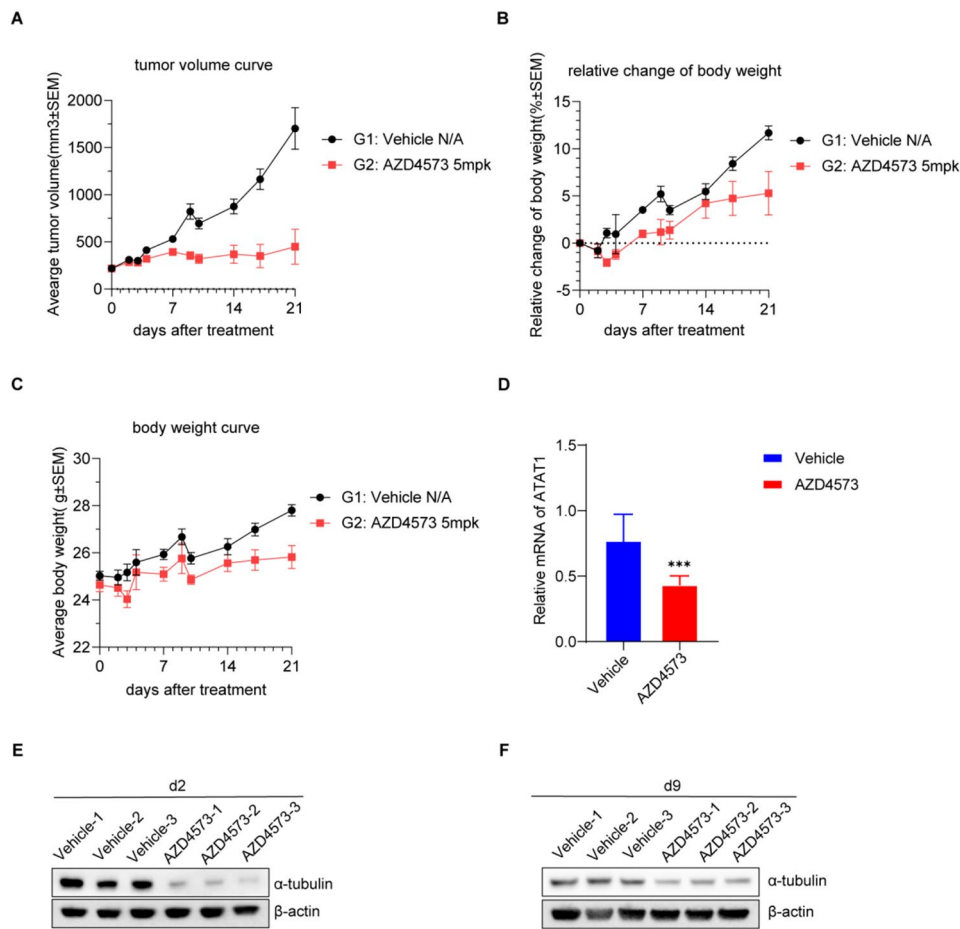


Fig. 7 Efficacy study of AZD4573 on MV4-11 model. **(A)** An MV4-11 subcutaneous xenograft model was treated with three cycles of vehicle or AZD4573 (5 mg/kg BID, 2 days on/5 days off). Tumor volumes are presented as geometric mean \pm SEM ($n=6$). **(B-C)** The body weight of mice was closely monitored. **(D)** MV4-11 tumors were harvested on day 2 (4 h after dosing). mRNA level of ATAT1 was tested using qPCR. The P-value was calculated via a t test, ***, $P < 0.001$. **(E-F)** MV4-11 tumors were harvested on days 2 **(E)** and 9 **(F)** (4 h after dosing). Protein levels of α -tubulin were tested by Western Blot

ATAT1 regulation, a mechanism that holds potential for future anti-cancer strategies. This novel insight also raises compelling questions regarding the specifics of how CDK9 modulates ATAT1, an area that requires in-depth future exploration.

Despite these promising findings, we acknowledge several limitations of our study. The exact mechanism by which CDK9 inhibition affects ATAT1 remains unclear. The complexities and diversities of malignant tumors often necessitate combination therapy for maximum therapeutic benefits, as monotherapies often lead to adaptive resistance over time. Additionally, potential neurotoxicity resulting from the combined application of CDK9 inhibitors and microtubule modulators like Vincristine necessitates careful assessment.

Our ongoing research aims to address these limitations, and further explores the potential of combining CDK9 inhibitors with other anti-tumor drugs to optimize therapeutic effects. As we strive for more precise cancer treatment strategies, we believe our findings contribute

significantly to understanding the novel targets and mechanisms of CDK9, offering new possibilities for cancer therapeutics.

This study has identified a novel function of CDK9 inhibitors for the first time. Given the crucial role of microtubules in various biological functions of cells, this discovery is significant for further understanding the mechanisms of CDK9 inhibitors and expanding our knowledge of microtubule metabolism.

Materials and methods

Chemicals

AZD4573 was purchased from MCE (MedChemExpress, China). JSH-105 was purchased from TargetMol Chemicals Inc (USA). For in vitro assays, this compound was solubilized to 10 mM in dimethyl sulfoxide (DMSO) and prepared to yield a final DMSO concentration of $< 0.3\%$. For in vivo studies, AZD4573 was prepared in a 2%/30%/68% mix of N, N-dimethylacetamide, PEG-400, and 1% (v/v) Tween-80.

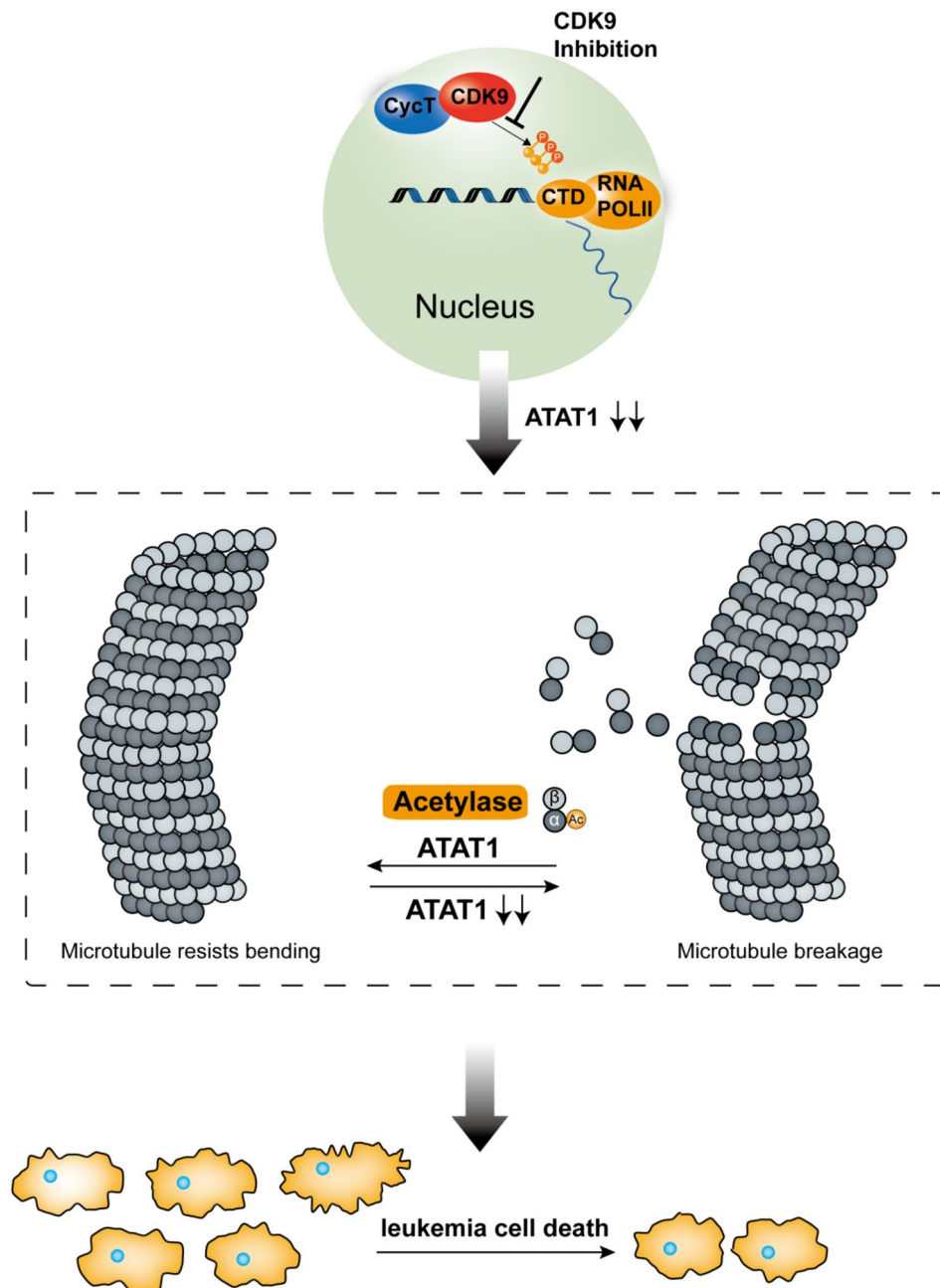


Fig. 8 CDK9 Inhibition reduces α -tubulin stability: A potential mechanism in cancer treatment. CDK9 inhibition downregulated the expression of ATAT1, the acetyltransferase responsible for α -tubulin acetylation, further compromising microtubule stability

Antibodies and reagents

The following antibodies were used for western blot: Cleaved PARP (Asp214) (D64E10) XP[®] Rabbit mAb (#5625,1:1000, Cell Signaling Technology, USA), CDK9 (C12F7) Rabbit mAb (#2316S,1:1000, Cell Signaling Technology, USA), Acetyl- α -Tubulin (Lys40) (D20G3) (#5335S,1:1000, Cell Signaling Technology, USA), HA-Tag (C29F4) Rabbit mAb (#3724,1:1000, Cell Signaling Technology, USA), Anti-rabbit IgG, HRP-linked Antibody (#7074,1:1000, Cell Signaling Technology, USA),

C6orf134 Polyclonal antibody (28828-1-AP,1:1000, Proteintech, China), Phospho-Rpb1 CTD (Ser2) (E1Z3G) Rabbit mAb (#13499S, 1:1000, Cell Signaling Technology, USA), HRP-conjugated Alpha Tubulin Monoclonal antibody (HRP-66031,1:5000, Proteintech, China), HRP-conjugated Beta Actin Monoclonal antibody (HRP-60008,1:5000, Proteintech, China), and HRP-conjugated GAPDH Monoclonal antibody (HRP-60004,1:5000, Proteintech, China). Other antibodies were utilized for immunofluorescence assays, including: Alpha Tubulin

Monoclonal antibody (66031-1-Ig,1:100, Proteintech, China), Acetyl- α -Tubulin (Lys40) (D20G3) (#5335S,1:500, Cell Signaling Technology, USA), Anti-rabbit IgG (H+L), F(ab')₂ Fragment (Alexa Fluor[®] 488 Conjugate) (#4412,1:1000, Cell Signaling Technology, USA), and Anti-rabbit IgG (H+L), F(ab')₂ Fragment (Alexa Fluor[®] 555 Conjugate) (#4413,1:1000, Cell Signaling Technology, USA).

Cell culture techniques

The following AML cell lines were used in this study: MOLM-13, MV4-11, OCI-AML3, THP-1, SUP-B15, RS4-11 (ATCC, USA). Cells were cultured in RPMI-1640 medium (Gibco, USA) containing 10% FBS, 100 U/mL penicillin/streptomycin, and maintained in a humidified incubator at 37 °C with 5% CO₂.

Plasmids and shRNA

Two CDK9 shRNA sequences (sh-CDK9-1: 5'-CCGGG CACAGTTTGGTCCGTTAGAACTCGAGTTCTAACG GACCAAACCTGTGCTTTTTG-3', sh-CDK9-2: 5'-CCG GCTACTACATCCACAGAAACAACCTCGAGTTGTTT CTGTGGATGTAGTAGTTTTTG-3') were transduced by lentivirus into AML cell lines to establish stable CDK9 KD cell lines.

For ATAT1 KD stable cell lines, two ATAT1 shRNA sequences (sh-ATAT1-1: 5'-GATCGGAAGGCTTCTT TGCCCATCAATCAAGAGTTGATGGGCAAAGAAG CCTTCTTTTT-3', sh-ATAT1-2: 5'-GATCGGATGATC GTGAGGCTCATAATTCAAGAGATTATGAGCCTCA CGATCATCTTTTT-3') were used via lentiviral transduction. pLVX-3HA- α -tubulin-WT-GFP-Puro plasmid, pLVX-3HA- α -tubulin-K40Q-GFP-Puro plasmid, and pLVX-3HA- α -tubulin-K40R-GFP-Puro plasmid were purchased from Shanghai Gengsi Biotechnology Co., Ltd. pLV2-CMV-Myc-ATAT1-Puro plasmid was purchased from Wenzhou Kemiao Biotechnology Co., Ltd. These plasmids were transduced by lentivirus into AML cell lines to establish stable overexpression cell lines.

Western blot

Protein samples were extracted from cell lines and tumors using RIPA lysis buffer. Protein quantitation was performed using a BCA kit (Thermo Fisher Scientific, USA). The samples were then mixed with 4 \times Laemmli blue loading buffer (Bio-Rad, USA) for electrophoresis. After transferring, primary antibodies were incubated with the samples overnight at 4 °C. Subsequently, secondary antibodies were used in a 1-hour incubation at room temperature. The blotting membranes were visualized using ECL reagent (Bio-Rad, USA) and exposure was carried out using ChemiDoc MP (Bio-Rad, USA). Western blot results were analyzed using Image lab software (Bio-Rad, USA).

Cell viability assay

The CellTiter Glo[®] Luminescent Cell Viability Assay was performed as described previously [26]. Cells were seeded into 96-well cell culture plates at a density of 5000 cells per well and treated with different concentrations of the indicated drugs. After 48 h of incubation, CellTiter Glo reagent (#G7573, Promega, USA) was used to lyse the cells, and the luminescence signals produced by ATP molecules from live cells were measured using the Variskin Flash plate reader (Thermo Fisher Scientific, USA) after a 25-minute incubation at room temperature.

Real-time polymerase chain reaction (RT-qPCR)

Total RNA from cell samples and tumors was extracted using RNAiso Plus Reagent (Takara, Japan), and reverse transcription was performed using HiScript III RT Super-Mix (Vazyme, China). Gene expression levels were determined using corresponding primers and the ChamQ SYBR qPCR Master Mix (Low ROX Premixed) (Vazyme, China) on the 7500 real-time PCR system (ABI). The comparative Ct approach was used to calculate the relative expression levels. For a list of primers used in this study, please refer to Table S1.

Immunofluorescence assay

The cells were bound to a glass slide surface at 4 °C for 30 min and fixed with 4% paraformaldehyde (Biossci, China) for 15 min. To permeabilize the cells, 0.5% Triton X was used. The cells were blocked with 10% goat serum in PBS for at least 1 h at room temperature. Primary antibodies were added to the cells and incubated overnight at 4 °C. On the following day, cells were incubated with Hoechst 33,342 (#B2261, Sigma Aldrich, USA) and fluorescence secondary antibodies at room temperature for at least 1 h. The slides were covered with coverslips and sealed with fluorescence mounting medium (DAKO, USA) and then scanned using a fluorescence scanner (Leica).

Generation of AZD4573 resistant cells

To generate cells that were resistant to CDK9 inhibition, MOLM-13 and MV4-11 were treated for 6 months with gradually increasing concentrations of AZD4573. Cells were considered AZD4573-resistant when they were able to remain 90–100% viable in the presence of this 5-fold higher than IC₅₀ concentration of AZD4573.

In vivo studies

Subcutaneous xenografts: All animal studies were performed according to the protocols approved by the ethics committee of Shanghai Jiao Tong University School of Medicine (SJTU-SM), and were carried out in accordance with institutional guidelines (IACUC). Injected cell numbers for cell line xenografts are as follows: 5 \times 10⁶

for MV4-11. AZD4573 was dosed intraperitoneally (IP) at 5 mg/kg, twice daily (BID), on a 2 days on/5 days off schedule. For each treatment group, $n = 12$ mice.

Statistical analysis

Student's *t*-tests were used to compare the data, and all values are presented as Mean \pm SEM. Throughout the study, *P*-values less than 0.05 were considered significant, * $P < 0.05$, ** $P < 0.01$, *** $P < 0.001$, **** $P < 0.0001$. All experiments were repeated in triplicate, and all statistical analyses were performed using GraphPad Prism 8.0.

Supplementary Information

The online version contains supplementary material available at <https://doi.org/10.1186/s12935-024-03588-8>.

Supplementary Material 1

Acknowledgements

The authors thank Zheng Ruan for her assistance with fluorescence scan.

Author contributions

Conceptualization, Ruibao Ren, Ping Liu, Baoyuan Zhang and Xi Xie; Data curation, Donghe Li, Jiaming Gao, Rui Zhang and Yunying Yao; Formal analysis, Jiaming Gao; Funding acquisition, Ping Liu, Ruibao Ren and Bo Jiao; Methodology, Xi Xie, Baoyuan Zhang, Jiaoyang Li, Chenxuan Liu, Yuqing Dan, Pengfei Xu, Lei Yan, Xu Huang, Jiawei Nie, Wei Huang, Xinru Wang and Bo Jiao; Project administration, Ping Liu; Resources, Baoyuan Zhang; Software, Donghe Li; Supervision, Ping Liu and Ruibao Ren; Visualization, Lei Yan; Writing – original draft, Xi Xie. All authors reviewed the manuscript.

Funding

This work was supported by the Key Project of National Natural Science Foundation of China (No. 82230088 to R.R.), National Natural Science Foundation of China (No. 81970134, 82170111 to P. L., No. 82170147 to R.R., No. 81870112 to R.R., 81770171 to B.J.), Shanghai Science and Technology Development Funds (No. 20Z11900200 to R.R.), Shanghai Collaborative Innovation Program on Regenerative Medicine and Stem Cell Research (No. 2019CXJQ01 to R.R.), the Samuel Waxman Cancer Research Foundation (to R.R.), Shanghai Pujiang Program (No. 2021PJD043 to B.J.) and the Innovative Research Team of High-level Local Universities in Shanghai (to R.R. and B.J.).

Data availability

No datasets were generated or analysed during the current study.

Declarations

Competing interests

The authors declare no competing interests.

Received: 17 July 2024 / Accepted: 26 November 2024

Published online: 05 December 2024

References

- Mandal R, Becker S, Strebhardt K. Targeting CDK9 for Anti-cancer therapeutics. *Cancers (Basel)*. 2021. 13(9).
- Chen FX, Smith ER, Shilatifard A. Born to run: control of transcription elongation by RNA polymerase II. *Nat Rev Mol Cell Biol*. 2018;19(7):464–78.
- Fujinaga K, Huang F, Peterlin BM. P-TEFb: the master regulator of transcription elongation. *Mol Cell*. 2023;83(3):393–403.
- Krystof V, et al. Pharmacological targeting of CDK9 in cardiac hypertrophy. *Med Res Rev*. 2010;30(4):646–66.
- Bagger FO, et al. HemaExplorer: a database of mRNA expression profiles in normal and malignant haematopoiesis. *Nucleic Acids Res*. 2013;41(Database issue):D1034–9.
- Lee DJ, Zeidner JF. Cyclin-dependent kinase (CDK) 9 and 4/6 inhibitors in acute myeloid leukemia (AML): a promising therapeutic approach. *Expert Opin Investig Drugs*. 2019;28(11):989–1001.
- Boffo S, et al. CDK9 inhibitors in acute myeloid leukemia. *J Exp Clin Cancer Res*. 2018;37(1):36.
- Cidado J, et al. AZD4573 is a highly selective CDK9 inhibitor that suppresses MCL-1 and induces apoptosis in Hematologic Cancer cells. *Clin Cancer Res*. 2020;26(4):922–34.
- Janke C, Magiera MM. The tubulin code and its role in controlling microtubule properties and functions. *Nat Rev Mol Cell Biol*. 2020;21(6):307–26.
- Prosser SL, Pelletier L. Mitotic spindle assembly in animal cells: a fine balancing act. *Nat Rev Mol Cell Biol*. 2017;18(3):187–201.
- Ishikawa T. Structural biology of cytoplasmic and axonemal dyneins. *J Struct Biol*. 2012;179(2):229–34.
- Kelliher MT, Saunders HA, Wildonger J. Microtubule control of functional architecture in neurons. *Curr Opin Neurobiol*. 2019;57:39–45.
- Perez EA. Microtubule inhibitors: differentiating tubulin-inhibiting agents based on mechanisms of action, clinical activity, and resistance. *Mol Cancer Ther*. 2009;8(8):2086–95.
- Pellegrini F, Budman DR. Review: tubulin function, action of antitubulin drugs, and new drug development. *Cancer Invest*. 2005;23(3):264–73.
- Chu CW, et al. A novel acetylation of beta-tubulin by San modulates microtubule polymerization via down-regulating tubulin incorporation. *Mol Biol Cell*. 2011;22(4):448–56.
- Verhey KJ, Gaertig J. The tubulin code. *Cell Cycle*. 2007;6(17):2152–60.
- Prokop A. Microtubule regulation: transcending the tenet of K40 acetylation. *Curr Biol*. 2022;32(3):R126–8.
- Kim GW, et al. Mice lacking alpha-tubulin acetyltransferase 1 are viable but display alpha-tubulin acetylation deficiency and dentate gyrus distortion. *J Biol Chem*. 2013;288(28):20334–50.
- Eshun-Wilson L, et al. Effects of alpha-tubulin acetylation on microtubule structure and stability. *Proc Natl Acad Sci U S A*. 2019;116(21):10366–71.
- Nekooki-Machida Y, Hagiwara H. Role of tubulin acetylation in cellular functions and diseases. *Med Mol Morphol*. 2020;53(4):191–7.
- Portran D, et al. Tubulin acetylation protects long-lived microtubules against mechanical ageing. *Nat Cell Biol*. 2017;19(4):391–8.
- Coombes C, et al. Mechanism of microtubule lumen entry for the alpha-tubulin acetyltransferase enzyme alphaTAT1. *Proc Natl Acad Sci U S A*. 2016;113(46):E7176–84.
- Szyk A, et al. Molecular basis for age-dependent microtubule acetylation by tubulin acetyltransferase. *Cell*. 2014;157(6):1405–15.
- Hubbert C, et al. HDAC6 is a microtubule-associated deacetylase. *Nature*. 2002;417(6887):455–8.
- North BJ, et al. The human Sir2 ortholog, SIRT2, is an NAD⁺-dependent tubulin deacetylase. *Mol Cell*. 2003;11(2):437–44.
- Janke C, Montagnac G. Causes and consequences of Microtubule Acetylation. *Curr Biol*. 2017;27(23):R1287–92.
- Barlaam B, et al. Discovery of AZD4573, a potent and selective inhibitor of CDK9 that enables short duration of Target Engagement for the Treatment of Hematological Malignancies. *J Med Chem*. 2020;63(24):15564–90.
- Alcon C, Manzano-Munoz A, Montero J. A new CDK9 inhibitor on the Block to treat hematologic malignancies. *Clin Cancer Res*. 2020;26(4):761–3.

Publisher's note

Springer Nature remains neutral with regard to jurisdictional claims in published maps and institutional affiliations.